Engineering and Technology Journal
Journal homepage: https://etj.uotechnology.edu.iq

Stress Analysis of Transversely Loaded Isotropic Three-Dimensional Plates Using a Polynomial Shear Deformation Theory

Festus C. Onyeka[a,c], **B. O. Mama**[b*], **Chidobere D. Nwa-David**[c]

[a] Civil Engineering Dept., Faculty of Engineering, Edo State University, Edo State, Nigeria.
[b] Civil Engineering Dept., Faculty of Engineering, University of Nigeria, Enugu State, Nigeria.
[c] Civil Engineering Dept., Faculty of Engineering, Michael Okpara University of Agriculture, Umudike, Abia State, Nigeria.
*Corresponding author Email: Benjamin.mama@unn.edu.ng

HIGHLIGHTS

- A 3-D total potential energy was developed.
- A derived shape function of the plate was obtained.
- An expression for stress and moment of the plate was formulated.

ARTICLE INFO

Handling editor: Mahmoud S. Al-Khafaji

Keywords:
Three-dimensional plate theory
Fourth-order polynomial shear deformation and displacement function
Exact Solution for bending analysis
SCFC Thick Plate

ABSTRACT

An exact solution for the bending attributes of a thick rectangular plate under transverse loading is modeled herein using three-dimensional (3-D) elasticity plate theory and fourth-order polynomial shear deformation function. Precluding coefficients of shear correction, this model captured the effect of shear deformation along with the transverse normal strain stress. The expression for total potential energy was derived from a 3-D kinematic and constitutive relation the equilibrium equation was developed and employed from the energy functional transformation to get the relationship between slope and deflection. Exact polynomial functions were obtained from the outcome of the equilibrium equation and with the aid of the direct variation approach, the coefficient of deflection of the plate was generated from the governing equation. The expression for computing the displacement, bending moments, and stress components along the three axes of the plate was established from these solutions for the assessment of the bending characteristics of a rectangular plate. The result of a simply supported at one edge, free at one edge and clamped at the two outer edges (SCFC) was evaluated using the obtained functions in this study. The report of this study confirms the exactness and consistency of the 3-D model unlike the refined plate theories applied by previous authors in the available literature. The value of 8.05% is the comprehensive average percentage variation of the values for center deflection obtained by Onyeka and Okeke (2020) and Gwarah (2019). It is established that at the 92 % confidence level, this model is worthy of adoption for safe, cost-effective and accurate bending analysis of thick plates of any support condition.

1. Introduction

Plates are three-dimensional structural members having spatial dimensions along x, y, and z-axis whose thickness is geometrically less compared to other dimensions [1-2]. They are vastly applied in aeronautical, naval, mechanical, Geotechnical, and structural engineering for modeling water tanks, bridge deck slabs, turbine disks, ship hulls, retaining walls, machine parts, and architectural structures [3-5].

Plates can be classified according to shapes such as; quadrilateral, square, circular, or rectangular; they can be classified based on the integral constituents as homogeneous, non-homogeneous, orthotropic, anisotropic, or isotropic [6-7]. Considering boundary status, plates are fixed, free, or simply supported, and they can be thin, moderately thick, or thick based on the span-to-thickness ratio of the plate [8-10].

Rectangular plates $a/t \leq 20$ are addressed as thick plates, while $20 \leq a/t \leq 50$ as moderately-thick plates and $50 \leq a/t \leq 100$ as thin plates, where a/t is the span-to-depth ratio [11]; given a and t to be the width and thickness respectively. There is increasing research interest for thick plates in engineering structures among scholars due to their pertinence and captivating attributes, features such as lightweight, heavy loads carrying-capacities, cost reduction, high mechanical properties, and ability

http://doi.org/10.30684/etj.2023.137410.1345
Received 18 December 2022; Accepted 07 January 2023; Available online 22 January 2023
2412-0758/University of Technology-Iraq, Baghdad, Iraq

to be customized to the desired state [12]. The properties of thick plates can be improved with adequate perspicacity of its failure form and structural trait.

The investigation on thick plates can be generally and thoroughly made through bending, vibration or buckling [13-15]). The deformation of plates, due to the application of lateral loads or external forces on the plate, at right angles towards the surface of the plate is considered as a bending phenomenon. Deformation extends as the induced load exceeds the critical load [16-17]. This results in plate failure. This study is of great essence because the bending mannerism of thick plates requires adequate attention to circumvent structural instability emanating from deformations and obtain an exact solution.

Several theories such as the classical plate theory (CPT), refined plate theories (RPTs), and three-dimensional theory (3-D) [18] were formulated and deployed by diverse scholars to solve the plight of instability arising from bending. RPTs consist of the first-order shear deformation plate theory (FSDT) [19-20], the trigonometric shear deformation theories (TSDT) [21-22], exponential shear deformation theories (ESDT) [23], polynomial shear deformation theories (PSDT) [24] and the higher-order shear deformation plate theories (HSDT) [25-26]. An accurate solution for the bending of thick plates cannot be actualized using classical plate theory (CPT) [27] because it neglects transverse shear effects. Although RPTs give a better analytical result, their solution is incomplete and inconsistent as they overlook the normal stress and strain along the thickness axis of the plate.

The solutions of the 3D model are accurate and reliable as the limitations of 2D-RPT are terminated with the comprehensive system of fifteen governing equations which consists of material constitutive laws for generalized stress - strain equations, the kinematic relations for six strains and displacements and the three differential equations of equilibrium [28-30]. This study is needful as thick plate analysis is a three-dimensional problem and it is advantageous as it investigates thick plates with SCFC support order.

Studies on bending can be carried out numerically, analytically or using an energy approach or a miscellany of any [31]. In the analytical approach, the outcome of the bending issue covers the edge requirements of the plate in the governing equations at different positions of the plate surface. This method includes; Integral transforms, Eigen expansion, Naiver, and Levy series [1, 32], while the numerical approach whose solutions are approximate [33-34], consists of; Galerkin, Collocation, Bubnov-Galerkin, truncated double Fourier series, Kantorovich methods, boundary element, Ritz, and finite difference. The energy method whose total energy is equal to the sum of strain and potential energy or external work on the continuum [35]; can be in an analytical or a numerical form.

Unlike the preceding works, this study evaluates the deflection, shear stresses at the x-y axis, x-z axis, and y-z axis, the normal stresses along x, y, and z co-ordinates produced due to the applied load on the plate, as well as the in-plane displacement in the direction of x and y co-ordinates. Inexact solutions were obtained by past authors that employed assumed displacement-shape functions and others that used an exact process only applied to the solution of the 2-D bending problem of the thick plate. The nature of the shape functions used during analysis matters so much to the designer as it affects the applicability and performance of the structure; to enhance the robustness of the process and at the same time ensure structural integrity and accuracy of solutions in the plate bending problem, a 3-D polynomial theory is required. This study also addresses this gap by excellently combining RPT of fourth order polynomial with a 3-D elasticity plate theory which is an improvement to past works and more advantageous as it can easily be employed to analyze plates with any boundary condition. A thick plate that is subjected to a uniformly-distributed transverse loads, and simply supported at one edge, free at one edge and clamped at the two other edges (SCFC) was evaluated herein, using a 3-D polynomial plate theory and exact polynomial displacement function to determine the value of displacements, moments and stresses along x, y and z co-ordinate at arbitrary nodes of plates.

Bi-directional bending investigation of thick isotropic plates was carried out by Bhaskar et al., [36] using a new inverse TSDT and a finite element solution was developed, considering the effects of transverse shear deflection and rotating inertia. With the application of the dynamic version of the virtual work principle, the dominant equations and edge conditions of the theory were obtained. Although their model showed precise predictions of stresses-displacements when collated with other RPTs, it was unable to capture thick plates with SCFC-support order, polynomial functions, and an analytical and 3D approach.

Neglecting the use of shear correction elements connected with FSDTs, Sayyad and Ghugal [37], as well as Ghugal and Gajbhiye [38] captured the effect of shear and strain deformation in their bending study. The phenomenon of zero-shear transverse stresses was satisfactory. Polynomial displacement functions with 3D theory and SCFC plates were not considered in their assessment.

Simply-supported plates under transverse bi-sinusoidal loads were evaluated by Mantari and Soares [39] using the precept of virtual work and HSDT with an assumed variation of the mechanical properties of the plates in the thickness axis. The authors obtained a Navier-type analytical solution which showed a level of accuracy compared to the previous shear deformation model. The 3D theory and polynomial shape functions were not applied. Plates with SCFC edge status were not covered.

Both trigonometric and polynomial displacement functions were employed by Onyeka and Okeke [40] to formulate the governing differential equation for SSFS plates. They used the direct energy method in their bending analysis and the deflection and stresses obtained in their study were in good agreement with the other RPTs. 3-D theory and SCFC plates were not encapsulated in their study. Mantari et al. [41] employed trigonometric functions and shear deformation plate theory to obtain the displacement and stresses in the thick rectangular plates. The approach applied by the authors cannot be reliable for a thick plate analysis as they cannot give an exact solution. The authors did not apply 3D theory, neither were polynomial functions incorporated. Plates with SSFS support status were not addressed in their study. An alternate refined plate model was

developed by Onyeka *et al.,* [42] for analyzing the effect of bending CCFC thick plates using the energy method. The authors obtained exact solutions as 3-D kinematic and constitutive relations were applied to formulate the equilibrium equations and total energy function. The beauty of their analytical approach and solutions is undeniable but their model was not a blend of the polynomial RPT and the 3D plate theory rather a trigonometric displacement function was used. In addition, plates with SCFC edge status were not considered in their study.

The spline-collocation method with two-coordinate directions and a numerical approach based on the 3-D theory was employed by Grigorenko et al*.,* [43] to get the bending solutions of a thick plate. They determined the displacements-stresses in clamped plates. Their approach did not capture accurately the value for out-of-plane displacements at any given point in the plate. They did not cover plates with the SCFC support - condition. Onyeka et al. [1] and Onyeka and Mama [44] presented a 3D trigonometric model for CSCS and SSSS plates respectively. The authors solved the bending issue of these plates using a direct variational energy approach. The solutions obtained in their study validate the accuracy of 3D prediction. But a combination of 2D-RPT and 3D theory with the polynomial function was not considered in their study. Plates with the SCFC boundary condition were also not addressed.

Antecedently, refined plate theories were mostly used by many scholars in the bending investigation of rectangular plates while the 3D model was used by a few authors as shown in the available literature. The solutions obtained by those that employed 2D-RPTs were inexact because the stresses along the thickness axis were not analyzed. Although those who applied 3D theory had exact solutions, polynomial displacement-shape functions were not deployed. This study addressed these research gaps and distinctively presented the coalescence of 3-D and RPT of fourth-order polynomial function which was not seen in preceding studies. The assumed shape functions applied in prior studies birthed erroneous and unreliable solutions as the functions were not derived from the governing compatibility equation that was obtained from the first principle. Discordant to other studies that used trigonometric functions to proffer solutions to bending problems, this work utilized polynomial shape functions, which is an easy and simplified approach that can solve any boundary condition of thick plates. The importance and the application of this study is to achieve a more economic analysis by considering all parameters responsible for the deformation of the plate structure.

In this study, a theoretical formulation was developed using the principle of 3-D elasticity to achieve an exact bending solution for thick isotropic plates carrying uniformly distributed transverse loads. The solution of a rectangular plate with one simply supported edge, one free edge, and clamped at the two outer edges (SCFC), is presented using a derived polynomial model. Furthermore, the function of stresses, shear stresses, slope, and displacement at the three planes of the plate at different span - thickness ratios and aspect ratios of the plate were examined.

2. Theoretical Section

The model of this study was formulated by considering a rectangular plate in Figure 1 as a three-dimensional element in which the deformation exists in three-axisxis: length (a), width (b) and thickness (t).

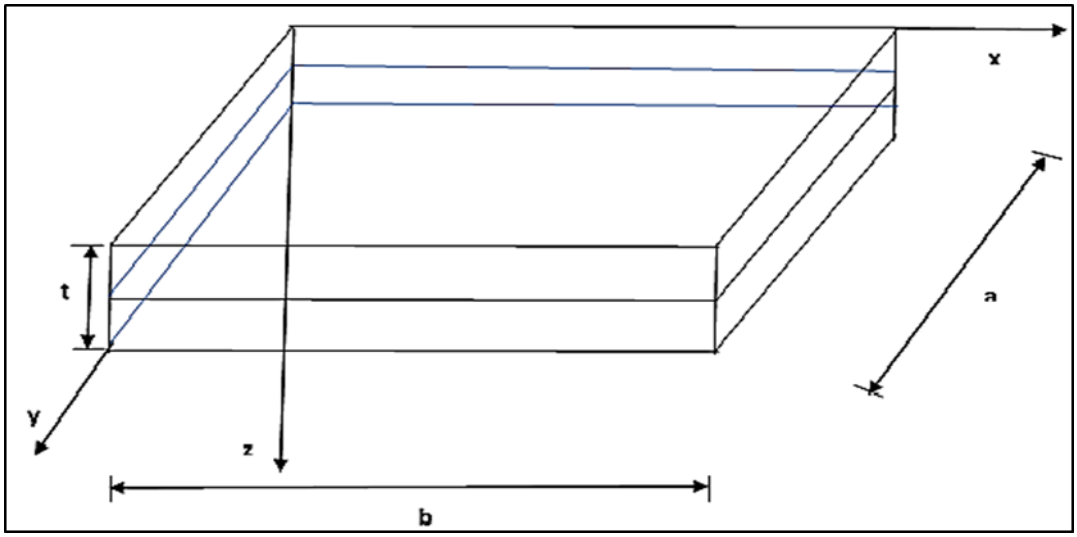

Figure 1: An element of thick rectangular plate showing middle surface

The displacement field which includes the displacements along x, y and z-axis: p, q and U are obtained assuming that the x-z section and y-z section, which are initially normal to the x-y plane before bending go off normal to the x-y plane after bending of the plate see Figure 2.

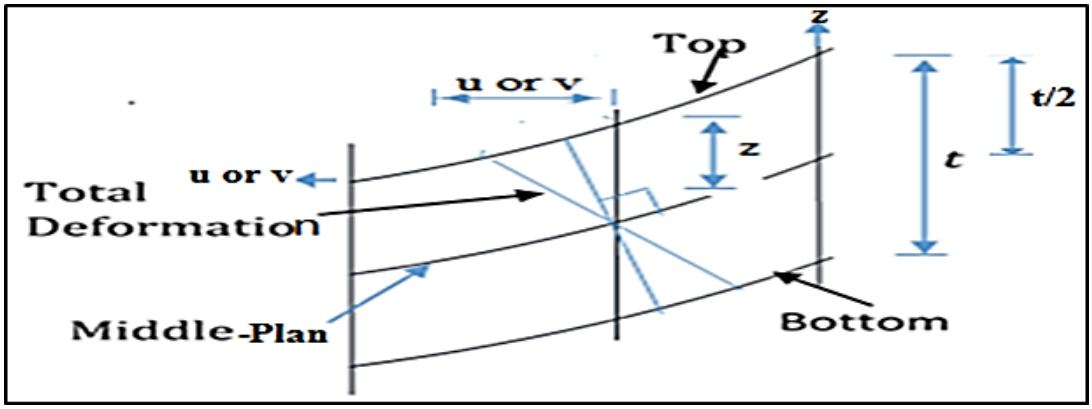

Figure 2: Displacement of x-z (or y-z) section after bending [4]

2.1 Kinematics

The kinematics of the study if formulated by taking the assumption of the plate that the x-z section and y-z section, is no longer normal to the x-y plane after bending. Thus, the 3-D displacement kinematics along x, y and z axis are obtained in line with the work of Onyeka et al. [2], as:

$$p = z.\emptyset_x \tag{1}$$

$$q = z.\emptyset_y \tag{2}$$

Given that:

$$z = kt \tag{3}$$

$$\beta = \frac{\mathrm{a}}{t} \tag{4}$$

$$\gamma = \frac{\mathrm{b}}{a} \tag{5}$$

All the used symbols are defined in the nomenclature section. Thus, the six non-dimensional coordinates strain components were derived using strain-displacement expression according to Hooke's law and presented in Equations (6) - (11):

$$\varepsilon_x = \frac{1}{\mathrm{a}}.\frac{\partial p}{\partial u} \tag{6}$$

$$\varepsilon_y = \frac{1}{\mathrm{a}\gamma}.\frac{\partial q}{\partial v} \tag{7}$$

$$\varepsilon_z = \frac{1}{\mathrm{t}}.\frac{\partial \cup}{\partial k} \tag{8}$$

$$\gamma_{xy} = \frac{1}{\mathrm{a}}.\frac{\partial q}{\partial u} + \frac{1}{\mathrm{a}\gamma}.\frac{\partial p}{\partial v} \tag{9}$$

$$\gamma_{xz} = \frac{1}{\mathrm{a}}.\frac{\partial \cup}{\partial u} + \frac{1}{\mathrm{t}}.\frac{\partial p}{\partial k} \tag{10}$$

$$\gamma_{yz} = \frac{1}{\mathrm{a}\gamma}.\frac{\partial \cup}{\partial v} + \frac{1}{\mathrm{t}}.\frac{\partial q}{\partial k} \tag{11}$$

2.2 Constitutive Relations

The three dimensional constitutive relation for isotropic material is given as [45]:

$$\begin{bmatrix}\varepsilon_x\\ \varepsilon_y\\ \varepsilon_z\\ \gamma_{xz}\\ \gamma_{yz}\\ \gamma_{xy}\end{bmatrix}=\frac{1}{E}\begin{bmatrix}1 & -\mu & -\mu & 0 & 0 & 0\\ -\mu & 1 & -\mu & 0 & 0 & 0\\ -\mu & -\mu & 1 & 0 & 0 & 0\\ 0 & 0 & 0 & 2(1+\mu) & 0 & 0\\ 0 & 0 & 0 & 0 & 2(1+\mu) & 0\\ 0 & 0 & 0 & 0 & 0 & 2(1+\mu)\end{bmatrix}\begin{bmatrix}\sigma_x\\ \sigma_y\\ \sigma_z\\ \tau_{xz}\\ \tau_{yz}\\ \tau_{xy}\end{bmatrix} \quad (12)$$

The six stress components were obtained by substituting Equations 6 to 11 into Equation 12 and simplifying the outcome gave:

$$\sigma_x=\left[\mu\frac{kt}{\gamma a}*\frac{\partial\emptyset_y}{\partial v}+(1-\mu)\ \frac{kt}{a}*\frac{\partial\emptyset_x}{\partial u}+\mu\frac{1}{t}*\frac{\partial\cup}{\partial k}\right]\frac{E}{(1+\mu)(1-2\mu)}(\quad (13)$$

$$\sigma_y=\left[\mu kt*\frac{\partial\emptyset_x}{a\partial u}+\frac{\mu}{t}*\frac{\partial\cup}{\partial k}+\frac{(1-\mu)kt}{\gamma a}*\frac{\partial\emptyset_y}{\partial v}\right]\frac{E}{(1+\mu)(1-2\mu)} \quad (14)$$

$$\sigma_z=\left[\frac{\mu kt}{\gamma a}*\frac{\partial\emptyset_y}{\partial v}+\frac{(1-\mu)}{t}*\frac{\partial\cup}{\partial k}+\mu kt*\frac{\partial\emptyset_x}{a\partial u}\right]\frac{E}{(1+\mu)(1-2\mu)} \quad (15)$$

$$\tau_{xy}=\left[\frac{kt\partial\emptyset_y}{a2\partial u}*\frac{kt}{2\gamma a}\frac{\partial\emptyset_x}{\partial v}\right]\frac{E(1-2\mu)}{(1+\mu)(1-2\mu)} \quad (16)$$

$$\tau_{yz}=\left[\frac{1}{a2\gamma}\frac{\partial\cup}{\partial Q}+\frac{\emptyset_y}{2}\right]\frac{(1-2\mu)E}{(1+\mu)(1-2\mu)} \quad (17)$$

$$\tau_{xz}=\left[\frac{1}{a}\frac{\partial\cup}{2\partial u}+\frac{\emptyset_x}{2}\right]\frac{(1-2\mu)E}{(1+\mu)(1-2\mu)} \quad (18)$$

2.3 Formulation of Energy

The potential energy which is the summation of all the external work done on the body of the material and strain energy generated due to the applied load on the plate is mathematically defined as:

$$\nexists=\in-\ni \quad (19)$$

Given that $\nexists$, $\in$ and $\ni$ are the potential energy, strain energy and external work-done on the plate respectively, let;

$$\ni=wab\cap\int_0^1\int_0^1\complement\,du\,dv \quad (20)$$

and;

$$\in=\frac{tab}{2}\int_0^1\int_0^1\int_{-0.5}^{0.5}\left(\sigma_x\varepsilon_x+\sigma_y\varepsilon_y+\sigma_z\varepsilon_z+\tau_{xy}\gamma_{xy}+\tau_{xz}\gamma_{xz}+\tau_{yz}\gamma_{yz}\right)du\,dv\,dk \quad (21)$$

The strain energy is presented as triple integration of the sum of dot product of stresses and strain, shear stresses and shear strain with respect to x, y and z axis of the plate. The domain (boundary) for x and y axis is between 0 and 1 while boundary for z axis is between 0 and 0.5, given that deflection occurs at mid-plane of the thickness of the plate. The symbol u, v and k represents non-dimensional form for x, y and z axis of the plane. Thus, substituting Equations 22 and 25 into Equation 24 to get the energy Equation as:

$$\nexists=\frac{Et^3\gamma}{24(1+\mu)(1-2\mu)}\int_0^1\int_0^1\left[\left(\frac{\partial\emptyset_y}{\partial u}\right)^2\frac{(1-2\mu)}{2}+\frac{1}{\gamma}\frac{\partial\emptyset_x}{\partial u}*\frac{\partial\emptyset_y}{\partial v}+\frac{(1-\mu)}{\gamma^2}\left(\frac{\partial\emptyset_y}{\partial v}\right)^2+\frac{(1-\mu)}{t^2}*\left(\frac{\partial\cup}{\partial k}\right)^2\beta^2+\frac{(1-2\mu)}{2\gamma^2}\left(\frac{\partial\emptyset_x}{\partial v}\right)^2+\frac{6(1-2\mu)}{t^2}\left\{a^2{\emptyset_x}^2+\left(\frac{\partial\cup}{\partial u}\right)^2+a^2{\emptyset_y}^2+\left(\frac{\partial\cup}{\partial v}\right)^2\frac{1}{\gamma^2}+a\left(\frac{\partial\cup}{\partial u}\right)2\emptyset_x+\left(\frac{\partial\cup}{\partial v}\right)2a*\frac{\emptyset_y}{\gamma}\right\}+\left(\frac{\partial\emptyset_x}{\partial u}\right)^2(1-\mu)\Bigg]\partial u\partial v\ -w\gamma a^2\int_0^1\int_0^1\complement S\,\partial u\partial v \quad (22)$$

2.4 Solution to The Equilibrium Equation

The two compatibility equations were obtained by minimizing the total potential energy functional with respect to rotations in x-z and in y-z plane to give:

$$\frac{Et^3\gamma}{24(1+\mu)(1-2\mu)}\int_0^1\int_0^1\left[\begin{matrix}2(1-\mu)\frac{\partial^2\emptyset_x}{\partial u^2}+\frac{\partial^2\emptyset_y}{\partial u\partial v}*\frac{1}{\gamma}+\frac{(1-2\mu)}{\gamma^2}\frac{\partial^2\emptyset_x}{\partial v^2}+\\ \left(2a^2\theta_{sx}+2a.\frac{\partial\cup}{\partial u}\right)\frac{6(1-2\mu)}{t^2}\end{matrix}\right]\partial u\partial v=0 \quad (23)$$

$$\frac{Et^3\gamma}{24(1+\mu)(1-2\mu)}\int_0^1\int_0^1\left[\begin{matrix}\frac{\partial^2\emptyset_x}{\partial u\partial v}*\frac{1}{\gamma}+2\frac{\partial^2\emptyset_y}{\partial v^2}*\frac{(1-\mu)}{\gamma^2}+2\frac{(1-2\mu)}{2}\frac{\partial^2\emptyset_y}{\partial u^2}+\\ \left(2a^2\emptyset_y+\frac{2a.}{\gamma}\frac{\partial\cup}{\partial v}\right)\frac{6(1-2\mu)}{t^2}\end{matrix}\right]\partial u\partial v=0 \quad (24)$$

The solution of the equilibrium differential equation gives the characteristics trigonometric displacement and rotation functions as presented in the Equation 25-27 as:

$$\cup = H_0[(1\ u\ u^2\ u^3\ u^4)\begin{bmatrix}a_0\\a_1\\a_2\\a_3\\a_4\end{bmatrix}.(1\ v\ v^2\ v^3\ v^4)\begin{bmatrix}b_0\\b_1\\b_2\\b_3\\b_4\end{bmatrix}] \quad (25)$$

$$\emptyset_x=\frac{c}{a}.H_0[(1\ 2R\ 3R^2\ 4R^3)\begin{bmatrix}a_1\\a_2\\a_3\\a_4\end{bmatrix}.(1\ Q\ Q^2\ Q^3\ Q^4)\begin{bmatrix}b_0\\b_1\\b_2\\b_3\\b_4\end{bmatrix}] \quad (26)$$

$$\emptyset_y=\frac{c}{a\beta}.H_0[(1\ R\ R^2\ R^3\ R^4)\begin{bmatrix}a_0\\a_1\\a_2\\a_3\\a_4\end{bmatrix}.(1\ 2Q\ 3Q^2\ 4Q^3)\begin{bmatrix}b_1\\b_2\\b_3\\b_4\end{bmatrix}] \quad (27)$$

A specific problem is presented in Figure 3 which contains a transversely loaded rectangular isotropic plate whose Poisson's ratio is 0.3 under uniformly distributed load as shown in the Figure 3. The plate has three dimensions; width (a), length (b) and thickness (t) which is situated along the direction of x, y and z co-ordinate under SCFC boundary condition to get the particular solution of the deflection. The symbol u, v and k represents non-dimensional form for x, y and z planes of the plate as seen in the figure below.

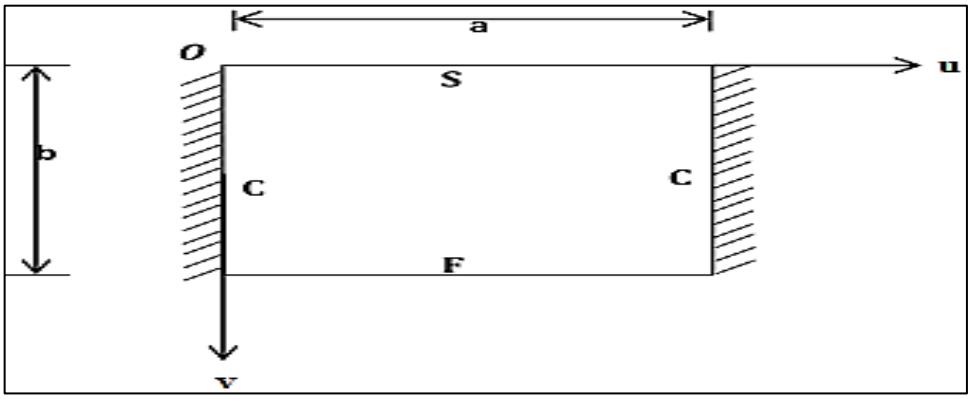

Figure 3: SCFC Rectangular Plate

Applying the initial conditions of the plate in Figure 2, the relationship between the displacement and shape function of the plate as:

$$\cup = C.\cap \quad (28)$$

$$\emptyset_x=\frac{h}{a}.\frac{\partial C}{\partial u} \quad (29)$$

$$\emptyset_y=\frac{g}{\gamma a}.\frac{\partial C}{\partial v} \quad (30)$$

The in trigonometric form of the shape function of the plate after satisfying the boundary conditions is given as:

$$\mathrm{C}= (R^2 - 2R^3 + R^4) \times \left(\frac{7Q}{3} - \frac{10}{3}Q^3 + \frac{10}{3}Q^4 - Q^5\right) \tag{31}$$

Substituting Equation 28, 29 and 30 into 22, gives:

$$\nexists = \frac{\mathrm{Et}^3\gamma}{24(1+\mu)(1-2\mu)}\left[(1-\mu)h^2 r_x + \frac{1}{\gamma^2}\left[h.g + \frac{(1-2\mu)h^2}{2} + \frac{(1-2\mu)g^2}{2}\right]r_{xy} + \frac{(1-\mu)g^2}{\gamma^4}r_y + 6(1-2\mu)\beta^2\left([h^2 + \cap^2 + 2\cap h].r_z + \frac{1}{\gamma^2}.[g^2 + \cap^2 + 2\cap g].r_{2z}\right) - \frac{2qa^4 r_c \cap}{D^*}\right] \tag{32}$$

Where:

$$r_x = \int_0^1\int_0^1\left(\frac{\partial^2 \mathrm{C}}{\partial u^2}\right)^2 \partial u \partial v \tag{33}$$

$$r_{xy} = \int_0^1\int_0^1\left(\frac{\partial^2 \mathrm{C}}{\partial u \partial v}\right)^2 \partial u \partial v \tag{34}$$

$$r_y = \int_0^1\int_0^1\left(\frac{\partial^2 \mathrm{C}}{\partial v^2}\right)^2 \partial u \partial v \tag{35}$$

$$r_z = \int_0^1\int_0^1\left(\frac{\partial \mathrm{C}}{\partial u}\right)^2 \partial u \partial v \tag{36}$$

$$r_{2z} = \int_0^1\int_0^1\left(\frac{\partial \mathrm{C}}{\partial v}\right)^2 \partial u \partial v \tag{37}$$

$$r_c = \int_0^1\int_0^1 \mathrm{C}\, \partial u \partial v \tag{38}$$

Minimizing Equation 32 with respect to h gives:

$$\frac{1}{2\gamma^2}[g + h(1-2\mu)]r_{xy} + hr_x(1-\mu) = -6(1-2\mu)\beta^2[h + \cap].r_z \tag{39}$$

Minimizing Equation 32 with respect to g gives:

$$\frac{1}{2\gamma^2}[h + g(1-2\mu)]r_{xy} + \frac{(1-\mu)g}{\gamma^4}k_y = +\frac{6}{\gamma^2}(1-2\mu)\beta^2([g + \cap].r_{2z}) \tag{40}$$

Re-write the Equation (39) and (40) and simplifying to give:

$$h = \cap\frac{(k_{12}k_{23} - k_{13}k_{22})}{(k_{12}k_{12} - k_{11}k_{22})} \tag{41}$$

$$g = \cap\frac{(k_{12}k_{13} - k_{11}k_{23})}{(k_{12}k_{12} - k_{11}k_{22})} \tag{42}$$

Where;

$$k_{11} = (1-\mu)r_x + \frac{1}{2\gamma^2}(1-2\mu)r_{xy} + 6(1-2\mu)\beta^2 r_z \tag{43}$$

$$k_{12} = k_{21} = \frac{1}{2\gamma^2}r_{xy};\ k_{13} = -6(1-2\mu)\beta^2 r_z \tag{44}$$

$$k_{22} = \frac{(1-\mu)}{\gamma^4}r_y + \frac{1}{2\gamma^2}(1-2\mu)r_{xy} + \frac{6}{\gamma^2}(1-2\mu)\beta^2 r_{2z} \tag{45}$$

$$k_{23} = k_{32} = -\frac{6}{\gamma^2}(1-2\mu)\beta^2 r_{2z} \tag{46}$$

Minimizing Equation 32 with respect to ∩ gives:

$$\frac{\mathrm{Et}^3\gamma}{24(1+\mu)(1-2\mu)}\left[6(1-2\mu)\beta^2\left([2\cap+2h].r_z+\frac{1}{\gamma^2}.[2\cap+2g].r_{2z}\right)\right] - \frac{24wa^4r_c(1+\mu)(1-2\mu)}{\mathrm{Et}^3}=0 \quad (47)$$

$$\frac{(1-2\mu)\beta^2\mathrm{Et}^3\gamma}{4(1+\mu)(1-2\mu)}\left\{\left[\cap+\cap\frac{(k_{12}k_{23}-k_{13}k_{22})}{(k_{12}k_{12}-k_{11}k_{22})}\right].r_z+\frac{1}{\beta^2}.\left[\cap+\cap\frac{(k_{12}k_{13}-k_{11}k_{23})}{(k_{12}k_{12}-k_{11}k_{22})}\right].r_{2z}\right\} = \frac{wa^4r_c(1+\mu)(1-2\mu)\beta^3}{\mathrm{E}} \quad (48)$$

Factorizing Equations (48) and simplifying gives:

$$\cap=\frac{2q(1+\mu)(1-2\mu)\beta^3}{E}\left\{\frac{ar_c}{(1-2\mu)\left(\frac{a}{t}\right)^2\left(\left[1+\frac{(k_{12}k_{23}-k_{13}k_{22})}{(k_{12}k_{12}-k_{11}k_{22})}\right].r_z+\frac{1}{\beta^2}.\left[1+\frac{(k_{12}k_{13}-k_{11}k_{23})}{(k_{12}k_{12}-k_{11}k_{22})}\right].r_{2z}\right)}\right\} \quad (49)$$

2.5 Exact Displacement and Stress Expression

By substituting the value of ∩ in Equation 49 into Equation 28, the deflection equation after satisfying the boundary condition of SCFC plate is given as:

$$\cup=\cap\left(R^2-2R^3+R^4\right)\times\left(\frac{7Q}{3}-\frac{10}{3}Q^3+\frac{10}{3}Q^4-Q^5\right) \quad (50)$$

Similarly, the in-plane displacement along x-axis becomes:

$$p=\frac{(k_{12}k_{23}-k_{13}k_{22})}{(k_{12}k_{12}-k_{11}k_{22})}\left\{\frac{12q(1+\mu)(1-2\mu)\beta^2kr_c}{(1-2\mu)\left(\frac{a}{t}\right)^2\left(\left[1+\frac{(k_{12}k_{23}-k_{13}k_{22})}{(k_{12}k_{12}-k_{11}k_{22})}\right].r_z+\frac{1}{\beta^2}.\left[1+\frac{(k_{12}k_{13}-k_{11}k_{23})}{(k_{12}k_{12}-k_{11}k_{22})}\right].r_{2z}\right)}\right\}\frac{1}{E}\frac{\partial \mathrm{C}}{\partial u} \quad (51)$$

$$p=\frac{12q(1+\mu)(1-2\mu)\beta^2}{E}\left(\frac{kMr_c}{L}\right)\frac{\partial \mathrm{C}}{\partial u} \quad (52)$$

Where;

$$L=6(1-2\mu)\beta^2\left([1+h].r_z+\frac{1}{\gamma^2}.[1+g].r_{2z}\right) \quad (53)$$

$$N=\frac{(r_{12}r_{23}-r_{13}r_{22})}{(r_{12}r_{12}-r_{11}r_{22})} \quad (54)$$

$$M=\frac{(r_{12}r_{13}-r_{11}r_{23})}{(r_{12}r_{12}-r_{11}r_{22})} \quad (55)$$

Similarly, the in-plane displacement along y-axis becomes;

$$q=\frac{12q(1+\mu)(1-2\mu)\beta}{E}\left(\frac{kNr_c}{L}\right)\frac{\partial \mathrm{C}}{\partial v} \quad (56)$$

The six stress elements after satisfying the boundary condition are presented in Equations (57) – (62) as:

$$\sigma_x=\frac{\mathrm{E}}{(1+\mu)(1-2\mu)}\left[\frac{\mathrm{k}}{\beta}.\frac{\partial^2 \mathrm{C}}{\partial u^2}(1-\mu)+\mu\beta^4*\frac{12q(1+\mu)(1-2\mu)}{E}\left(\frac{r_c}{L}\right)\frac{\partial \mathrm{C}}{\partial \mathrm{k}}+\frac{\mu\mathrm{k}}{\gamma\beta}.\frac{\partial^2 \mathrm{C}}{\partial v^2}\right] \quad (57)$$

$$\sigma_y=\frac{\mathrm{E}}{(1+\mu)(1-2\mu)}\left[\frac{\mu\mathrm{k}}{\beta}.\frac{\partial^2 \mathrm{C}}{\partial u^2}+\mu\beta^4*\frac{12q(1+\mu)(1-2\mu)}{E}\left(\frac{r_c}{L}\right)\frac{\partial \mathrm{C}}{\partial \mathrm{k}}+\frac{(1-\mu)\mathrm{k}}{\gamma\beta}.\frac{\partial^2 \mathrm{C}}{\partial v^2}\right] \quad (58)$$

$$\sigma_z = \frac{\mathrm{E}}{(1+\mu)(1-2\mu)}\left[\frac{\mu k}{\beta}.\frac{\partial^2 C}{\partial u^2} + (1-\mu)\beta^4 * \frac{12q(1+\mu)(1-2\mu)}{\beta}\left(\frac{r_c}{L}\right)\frac{\partial C}{\partial k} + \frac{\mu k}{\gamma\beta}.\frac{\partial^2 C}{\partial v^2}\right] \quad (59)$$

$$\tau_{xy} = \frac{E(1-2\mu)}{(1+\mu)(1-2\mu)}.\left[\frac{k}{2\beta}.\frac{\partial^2 \partial C}{\partial u\,\partial v} + \frac{\beta^2 k}{2a\gamma}.\frac{12q(1+\mu)(1-2\mu)}{E}\left(\frac{r_c}{L}\right)\frac{\partial^2 \partial C}{\partial u\,\partial v}\right] \quad (60)$$

$$\tau_{xz} = \frac{(1-2\mu)E}{(1+\mu)(1-2\mu)}.\left[\frac{1}{2}\frac{\partial C}{\partial u} + \frac{\beta^3}{2} * \frac{12q(1+\mu)(1-2\mu)}{E}\left(\frac{r_c}{L}\right)\frac{\partial C}{\partial u}\right] \quad (61)$$

$$\tau_{yz} = \frac{(1-2\mu)E}{(1+\mu)(1-2\mu)}.\left[\frac{1}{2}\frac{\partial C}{\partial v} + \frac{\beta^3}{2\gamma} * \frac{12q(1+\mu)(1-2\mu)}{E}\left(\frac{r_c}{L}\right)\frac{\partial C}{\partial v}\right] \quad (62)$$

3. Results and Discussion

A 3-D polynomial shear deformation model was developed to obtain the numerical outcome for the non-dimensional values of displacements, perpendicular and shear stresses of SCFC thick plate subjected to a transverse load. The variation of the displacements and stresses in a different span-depth ratio at varying length-breadth ratio, was presented in Tables 1 to 3 and Figures 4 to 12. The range of span-thickness ratio is considered between 4, 5, 10, 15, 20, 50, 100 and CPT, which covers the span of thick, moderately thick and thin plates. The length-breadth aspect ratio captured in this study is 1.0, 1.5 and 2.0.

Table 1: Displacement and Stresses of SCFC plate (length/width = 1)

$\propto = \frac{a}{t}$	∪	p	Q	$\overline{\sigma_x}$	$\overline{\sigma_y}$	$\overline{\sigma_z}$	$\overline{\tau_{xy}}$	$\overline{\tau_{xz}}$	$\overline{\tau_{yz}}$
4	0.0041	-0.0044	-0.0007	0.1551	-0.3106	0.0180	-0.0407	0.0191	0.0009
5	0.0034	-0.0040	-0.0006	0.1459	-0.2631	0.0170	-0.0358	0.0120	0.0005
10	0.0025	-0.0034	-0.0004	0.1350	-0.2002	0.0158	-0.0295	0.0029	0.0001
15	0.0024	-0.0033	-0.0004	0.1331	-0.1886	0.0156	-0.0283	0.0013	5E-05
20	0.0023	-0.0033	-0.0004	0.1325	-0.1846	0.0155	-0.0279	0.0007	3E-05
50	0.0023	-0.0033	-0.0004	0.1318	-0.1802	0.0154	-0.0275	0.0001	5E-06
100	0.0023	-0.0033	-0.0004	0.1317	-0.1795	0.0154	-0.0274	3E-05	1E-06
CPT	0.0023	-0.0033	-0.0004	0.1317	-0.1793	0.0154	-0.0274	3E-07	1E-08

Table 2: Displacement and Stresses of SCFC plate (length/width = 1.5)

$\propto = \frac{a}{t}$	∪	p	Q	$\overline{\sigma_x}$	$\overline{\sigma_y}$	$\overline{\sigma_z}$	$\overline{\tau_{xy}}$	$\overline{\tau_{xz}}$	$\overline{\tau_{yz}}$
4	0.0036	-0.0043	-0.00041	0.2173	-0.0813	-0.0129	-0.0329	0.0125	0.0003
5	0.0033	-0.0040	-0.00037	0.2068	-0.0714	-0.0104	-0.0304	0.0086	0.0002
10	0.0027	-0.0037	-0.00032	0.1919	-0.0570	-0.0270	0.0030	7.7E-05	-0.0270
15	0.0026	-0.0036	-0.00030	0.1874	-0.0525	-0.0259	0.0013	3.4E-05	-0.0259
20	0.0025	-0.0035	-0.00030	0.1859	-0.0510	-0.0255	0.0008	1.9E-05	-0.0255
50	0.0024	-0.0035	-0.00029	0.1842	-0.0493	0.0114	-0.0251	0.0001	2E-06
100	0.0024	-0.0035	-0.00029	0.1840	-0.0490	0.0114	-0.0251	3E-05	7.4E-07
CPT	0.0024	-0.0035	-0.00029	0.1839	-0.0490	0.0114	-0.0250	3E-07	7.4E-09

Table 3: Displacement and Stresses of SCFC plate (length/width = 2)

$\propto = \frac{a}{t}$	∪	p	Q	$\overline{\sigma_x}$	$\overline{\sigma_y}$	$\overline{\sigma_z}$	$\overline{\tau_{xy}}$	$\overline{\tau_{xz}}$	$\overline{\tau_{yz}}$
4	0.0043	-0.0048	-0.00037	0.2691	-0.0179	0.0180	-0.0288	0.0202	-0.0048
5	0.0036	-0.0044	-0.00031	0.2446	-0.0111	0.0170	-0.0253	0.0126	-0.0044
10	0.0027	-0.0038	-0.00025	0.2136	-0.0020	-0.0207	0.0031	-0.0038	-0.0207
15	0.0025	-0.0037	-0.00023	0.2080	-0.0002	-0.0199	0.0014	-0.0037	-0.0199
20	0.0024	-0.0036	-0.00023	0.2061	0.0004	-0.0196	0.0008	-0.0036	-0.0196
50	0.0024	-0.0036	-0.00022	0.2040	0.0010	0.0154	-0.0193	0.0001	-0.0036
100	0.0024	-0.0036	-0.00022	0.2037	0.0011	0.0154	-0.0192	3E-05	-0.0036
CPT	0.0024	-0.0036	-0.00022	0.2036	0.0011	0.0154	-0.0192	3E-07	-0.0036

The plot in Figures 4 to 6 showed that as the span-depth ratio increased, the out-of-plane displacements (∪) decreased positively while the in-plane displacements (p and q) increased negatively. Considering a span - depth ratio of 4 to 20, the result as presented in figures showed that the deflection values varied from 0.0041 & 0.0023, 0.0036 & 0.0025 and 0.0043 & 0.0024 at length-breadth ratio of 1.0, 1.5 and 2.0 respectively. It is observed that the value of deflection varies less as the span-depth ratio increases under the same loading capacity/condition. This implies that as the span of the plate is increasing, the deflection that will occur in the plate gradually goes higher. Plates at a span - depth ratio between 4 and 20 can be regarded as thick plates while span-thickness ratio of 50 and beyond can be considered as moderately-thick or thin plates as they are almost equivalent to the value of the CPT. The plate structure tends to fail when the reductions continues to the point where the deflection exceeds the elastic yield stress.

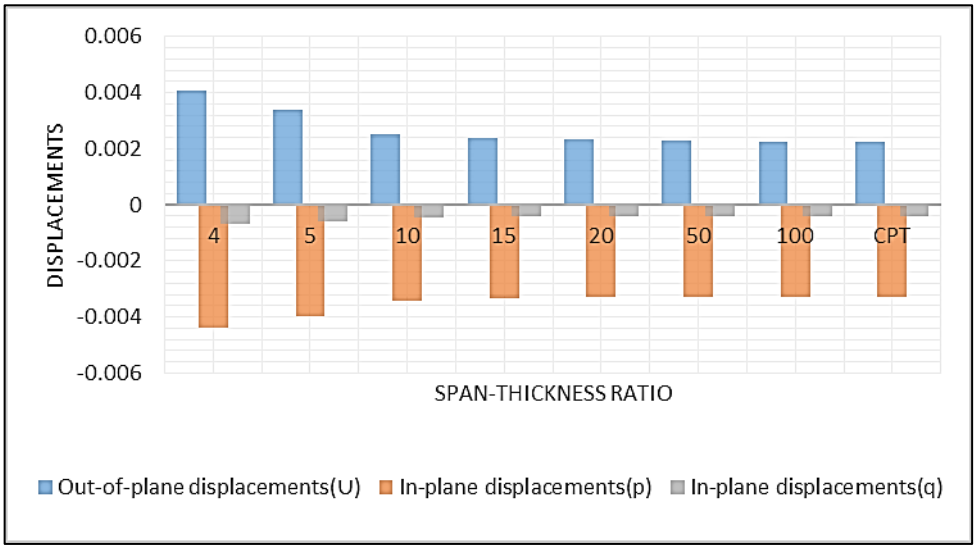

Figure 4: Displacements versus span-depth ratio of the plate at length-breadth ratio of 1.0

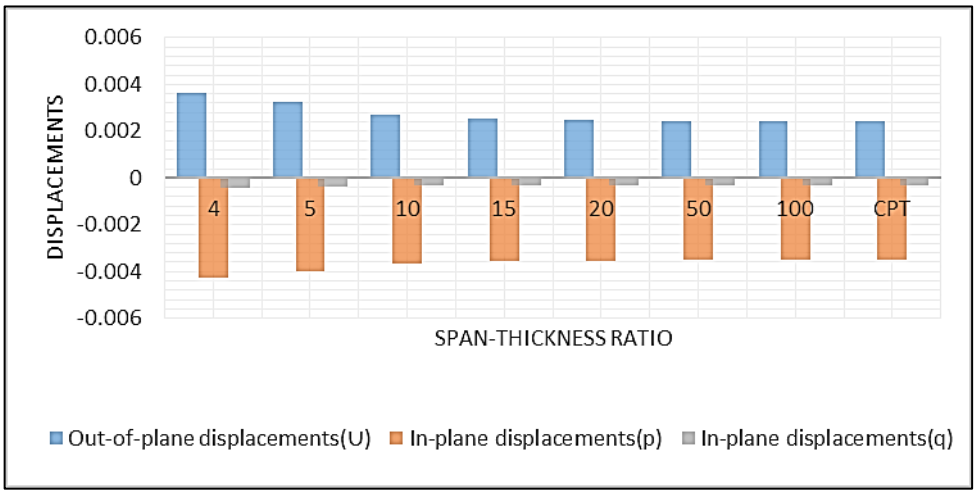

Figure 5: Displacements versus span-depth ratio of the plate at length-breadth ratio of 1.5

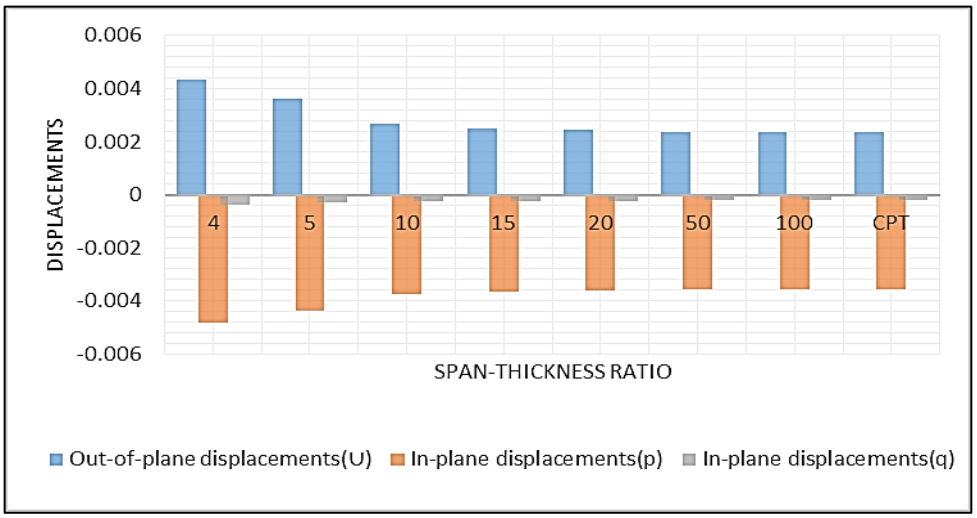

Figure 6: Displacements versus span-depth ratio of the plate at length-breadth ratio of 2.0

The stresses perpendicular to the x and z axis (σ_x, and σ_z) decreased positively while the ones in the y-axis (σ_y) increased negatively with an increase in span-thickness ratio, as shown in Figure 7. In Figure 8, the stresses perpendicular to the x-axis (σ_x) reduced positively while stresses perpendicular to the y-axis (σ_y) increased negatively as the span-depth ratio kept rising. Between span-depth ratios of 4 and 5, the normal stress in the z-plane (σ_z) increased negatively, dropped in the negative order at a span - depth ratio of 10 with a gradual negative increment till span-depth ratio of 20 and a constant value of 0.0114 at

span-depth ratio of 50 and beyond. The normal stresses in the x-axis (σ_x), as shown in Figure 9 decreased in the positive coordinate as the span-thickness ratio increased, perpendicular stresses in the y-axis (σ_y) increased negatively from span-depth ratio of 4 to 15 with a positive increase from span-depth of 20 to CPT. This implies that as the span of the plate is increasing, the stresses induced in the plate gradually goes higher. Figure 9 equally showed that stresses perpendicular to the z-axis (σ_z) dropped positively span-depth ratio of 4 and 5, with an increase in the negative sense between span-depth ratio of 10 till 20, maintaining a positive value of 0.0154 for span-depth ratio of 50, 100 and CPT.

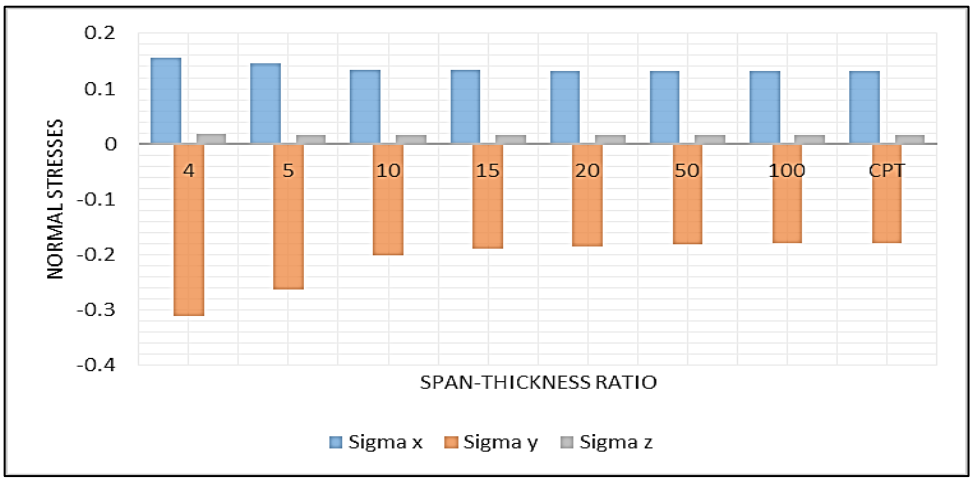

Figure 7: Normal stresses versus span-depth ratio of the plate at length-breadth ratio of 1.0

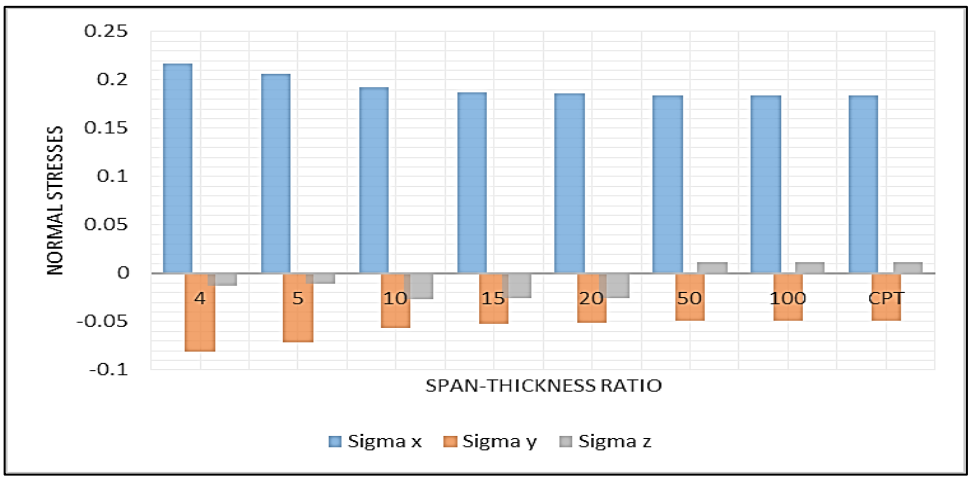

Figure 8: Normal stresses versus span-depth ratio of the plate at length-breadth ratio of 1.5

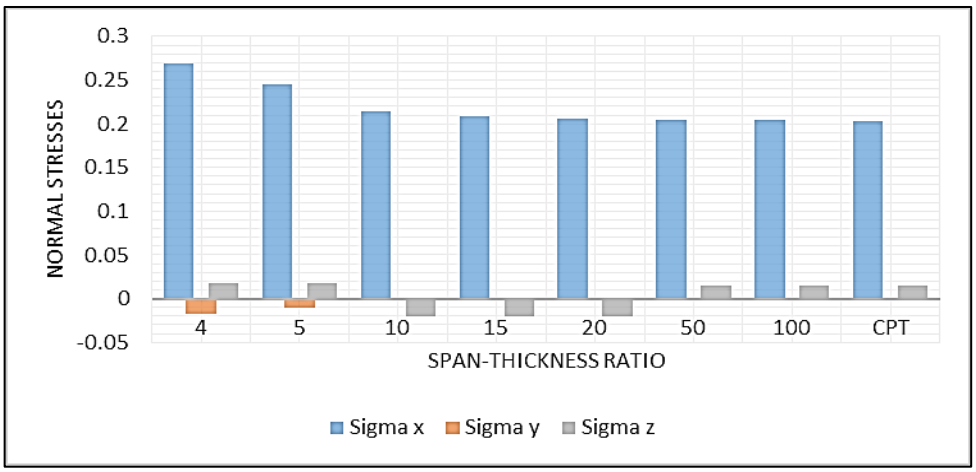

Figure 9: Normal stresses versus span-depth ratio of the plate at length-breadth ratio of 2.0

The non-dimensional parameters for the shear stresses in the in the x-y plane (τ_{xy}) increased in the negative order with each rise in the span - depth ratio and the shear stresses in the x-z, and y-z plane (τ_{xz} and τ_{yz}) reduced positively as presented in Figure 10. In Figure 11, there was a negative increase for the shear stresses in the x-y plane (τ_{xy}) for a span - depth ratio of 4 to

5 and 50 to CPT, with a reduction in the positive sense of span-depth ratio of 10 till 20. The same chart revealed the reduction of shear stresses in the x-z plane (τ_{xz}) positively. It also showed a positive reduction for span-depth ratio of 4 to 5, a negative rise in the span - depth ratio of 10 to 20 and a positive decrease for span-thickness ratio of 50 till CPT for shear stresses in the y-z plane (τ_{yz}). This implies that as the span (width) of the plate is increasing, the shearing stresses induced in the plate gradually goes higher even without increase of load in the plate material.

In Figure 12, shear stresses in the x-y plane (τ_{xy}) increased in the negative order from span-depth ratio of 4 to 5, with a positive reduction in the span - depth ratio of 10 till 20, and a constant negative value of 0.019 for a span - depth ratio of 50 till CPT. The same plot showed that there was a positive reduction in the shear stresses at x-z plane (τ_{xz}) for the span-depth ratio of 4 to 5, with a rise in the negative sense in span-depth ratio of 10 till 20 and a positive reduction of the values of the shear stresses. For span-depth ratio between 4 and 5, the values of the shear stresses in the y-z plane (τ_{yz}) increased negatively with the same occurrence at a span - depth ratio of 10 till 20 and had a constant negative value of 0.0036 for span-depth ratio of 50 and beyond.

In a nutshell, it can be deduced that there are categorically three rectangular plates. Plates whose deflection and transverse shear stress vary greatly from zero are considered as thick plates while thin plates can be categorized as plates whose vertical shear stress and deflection do not differ largely from zero; their values being almost the same as CPT values. Plates that lie in between the thick and thin plates are considered as moderately-thick plates. This attestation can be applied to depict the boundary between thin and thick plate. From this study, it can be inferred that thick plate is one whose span-depth ratio value is 4 up to 15.

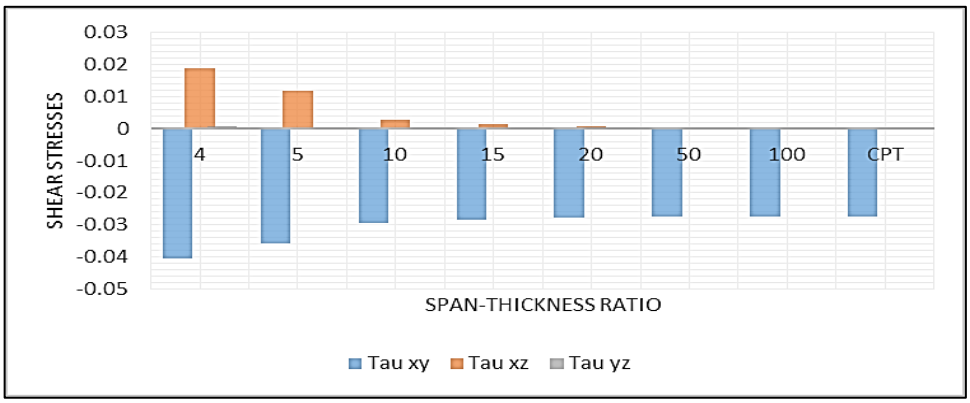

Figure 10: Shear stresses versus span-depth ratio of the plate at length-breadth ratio of 1.0

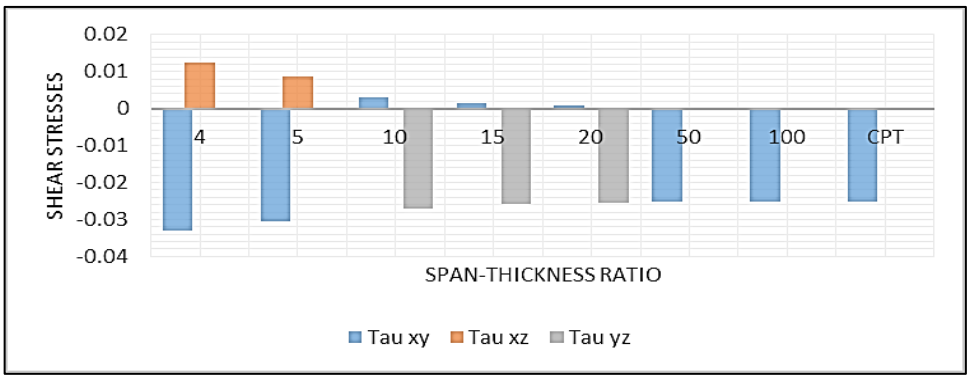

Figure 11: Shear stresses versus span-depth ratio of the plate at length-breadth ratio of 1.5

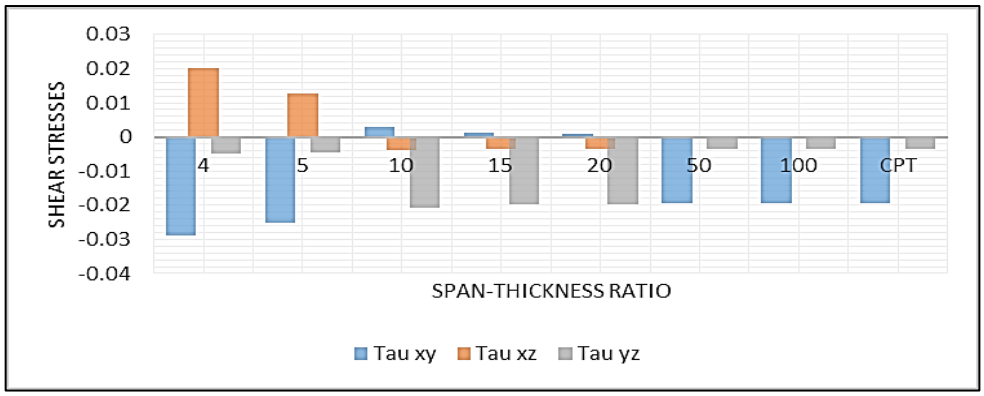

Figure 12: Shear stresses versus span-depth ratio of the plate at length-breadth ratio of 2.0

The result of the comparative evaluation tabulated in Table 4 and Figure 13 clearly showed the contrariety of this model and those of previous scholars. To validate the derived relationships in the deflection analysis, an assessment of the percentage difference was adopted and recorded in the table. As the span-depth ratio increased, it was observed that the non-dimensional values of deflection for both present and previous studies decreased. Table 4 and Figure 13 revealed that the study of Gwarah [47] varied about 6.8% from the present work while that of Onyeka and Okeke [46] about 9.6% from the present work. The reason for these variations is that both authors [46 and 47] applied refined plate theory which ofcourse uses 2-D analogy in the analysis. Significantly, both previous studies did not apply the amalgam of 3-D elasticity plate theory which proves to be responsible for the variation and inexact. This confirms the reliability of this model and the approach considered herein as it gives accurate and exact solutions. Plate is a typical 3-D element and should be analyzed as such. Thus, the present model is worth adopting for safe, cost-effective and accurate analysis of thick plates of any boundary condition. The overall percentage variation is 8.05%. This implies that the present study is equivalent to those of Onyeka and Okeke [46] and Gwarah [47] at 90.7% and 93.2% respectively. With this confidence level, the approach presented in this study may be espoused for adequate investigation of thick plates.

Table 4: Comparative central deflection analysis of square plate between present studies and past studies at different span-depth ratio

β = a/t	Present Work [P.W] (mm)	Onyeka and Okeke [46] (mm)	Gwarah [47] (mm)	Percentage difference between [P.W] & [46]	Percentage difference between [P.W] & [45]
4	0.004084	0.004465	0.003713	9.3291	9.0842
5	0.003407	0.003726	0.003147	9.3631	7.6313
10	0.002544	0.002786	0.002381	9.5126	6.4072
15	0.002389	0.002570	0.002238	7.5764	6.3206
20	0.002335	0.002559	0.002188	9.5931	6.2955
50	0.002277	0.002496	0.002134	9.6179	6.2802
100	0.002269	0.002487	0.002126	9.6078	6.3023
CPT	0.002266	0.002482	0.002123	9.5322	6.3107
		Average Percentage difference		9.27	6.83
		Total Percentage difference		8.05%	

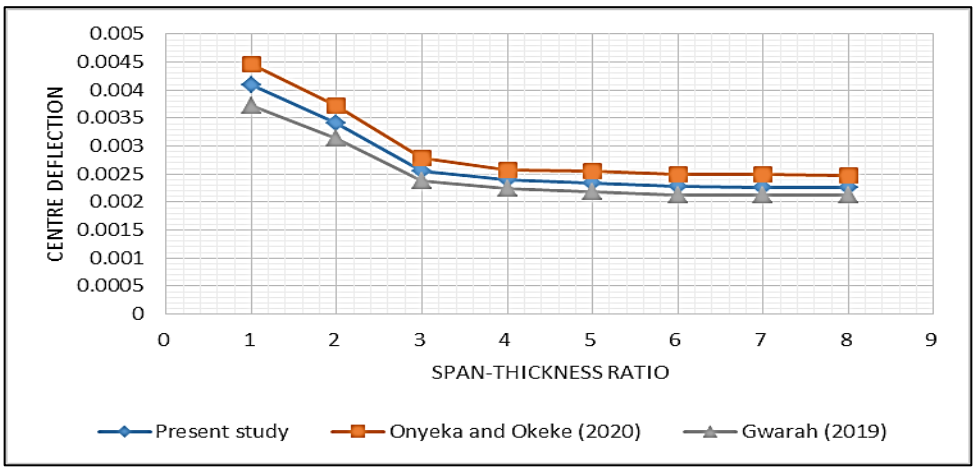

Figure 13: Comparative variation of deflection and span-depth ratios of present study and previous studies

4. Conclusion

The 3-D elasticity theory has been used to investigate the moments, displacements, and stresses of thick rectangular plates with the following conclusions drawn from it:

1) The result obtained in this work which are compared with those of previous works revealed that 2-D refined plate theories are quite coarse for thick plate analysis. RPTs under-estimates and over predicts stresses, displacements and bending loads within the engineering allowable error of 8.05% for thick plate analysis.
2) The model produced in this study can be employed to analyze plates at varying thicknesses.
3) The 3D elasticity solution gave a more accurate and reliable solution compared refined plate theories and are recommended for the analysis of thick plate under the initial condition.

Nomenclature

k	non-dimensional parameters of z-axis
u	non-dimensional parameters of x-axis
v	non-dimensional parameters of y-axis
t	thickness of the plate,
p	in-plane displacement along x-axis (mm)
q	in-plane displacement along y-axis (mm)
h	coefficient of shear deformation along x-axis of the plate
g	coefficient of shear deformation along y-axis of the plate
ε_x	normal strain along x-axis
ε_y	normal strain along y-axis
ε_z	normal strain along z-axis
γ_{xy}	shear strain in the plane parallel to the x-y plane
γ_{xz}	shear strain in the plane parallel to the x-z plane
γ_{yz}	shear strain in the plane parallel to the y-z plane
τ_{xy}	shear stress in the plane parallel to the x-y plane
τ_{xz}	shear stress in the plane parallel to the x-z plane
τ_{yz}	shear stress in the plane parallel to the y-z plane
E	modulus of elasticity
μ	Poisson's ratio
∄	Potential energy of the plate
∈	Strain energy of the plate
∋	External work done on the plate
⊂	Plate's shape function
w	Uniformly distributed load
∪	Deflection function of the plate
∩	Coefficient of deflection
$\emptyset_x$	Coefficient of shear deformation along x-axis
$\emptyset_y$	Coefficient of shear deformation along y-axis
β	Span-thickness ratio
α	Aspect ratio

Author contribution

All authors contributed equally to this work.

Funding

This research received no specific grant from any funding agency in the public, commercial, or not-for-profit sectors.

Data availability statement

Not applicable.

Conflicts of interest

The authors of the current work do not have conflict of interest .

References

[1] F. C. Onyeka, B. O. Mama, C. D. Nwa-David and T. E. Okeke, Exact analytic solution for static bending of 3-d plate under transverse loading, J. Comput. Appl. Mech., 53 (2022) 309-331. https://doi.org/10.22059/jcamech.2022.342953.721

[2] K. Chandrashekhara, Theory of plates. University Press (India) Limited, 2001.

[3] I. C. Onyechere, O. M. Ibearugbulem, C. U. Anya, K. O. Njoku, A. U. Igbojiaku , L. S. Gwarah, The use of polynomial deflection function in the analysis of thick plates using higher order shear deformation Theory, Saudi J. Civ. Eng., 4 (2020) 38-46. https://doi.org/10.36348/sjce.2020.v04i04.001

[4] F. C. Onyeka, B. O. Mama , C. D. Nwa-David . Application of Variation Method in Three-Dimensional Stability Analysis of Rectangular Plate Using Various Exact Shape Functions, Niger. J. Technol., 41 (2022) 8-20. https://doi.org/10.4314/njt.v41i1.2

[5] F. C. Onyeka, C. D. Nwa-David and E. E. Arinze, Structural imposed load analysis of isotropic rectangular plate carrying a uniformly distributed load using refined shear plate theory, FUOYE J. Eng. Technol., 6 (2021) 414-419. https://doi.org/10.46792/fuoyejet.v6i4.719

[6] J. N. Reddy, Classical theory of plates, In Theory and Analysis of Elastic Plates and Shells, CRC Press, 2006. https://doi.org/10.1201/9780849384165-7

[7] F. C. Onyeka ,T. E. Okeke, Application of higher order shear deformation theory in the analysis of thick rectangular plate. Int. j. Emerg. Technol., 11 (2020) 62-67.

[8] R. Szilard, Theories and Applications of Plates Analysis: Classical, Numerical and Engineering Methods, John Wiley and Sons Inc., 2004. https://doi.org/10.1002/9780470172872

[9] E. Ventsel ,T. Krauthammer, Thin plates and shells theory, analysis and applications, Maxwell Publishers Inc, New York , 2022.

[10] F. C. Onyeka, T. E. Okeke , C. D. Nwa-David, Static and buckling analysis of a three-dimensional (3-D) rectangular thick plates using exact polynomial displacement function, European J. Eng. Technol. Res.,7 (2022) 29-35. http://dx.doi.org/10.24018/ejeng.2022.7.2.2725

[11] F. C. Onyeka, B. O. Mama , C. D. Nwa-David. Analytical modelling of a three-dimensional (3D) rectangular plate using the exact solution approach, IOSR J. Mech. Civ. Eng., 19 (2022) 76-88. https://doi.org/10.9790/1684-1901017688

[12] F. C. Onyeka, F. O. Okafor and H. N. Onah, Buckling solution of a three-dimensional clamped rectangular thick plate using direct variational method, IOSR J. Mech. Civ. Eng., 18 (2021)10-22. https://doi.org/10.9790/1684-1803031022

[13] S. P. Timoshenko, J. M. Gere, Theory of elastic stability, 2nd Edition, McGraw-Hill Books Company, New York, 1963. https://doi.org/10.1115/1.3636481

[14] F. C. Onyeka, Critical lateral load analysis of rectangular plate considering shear deformation effect, Global J.Civ. Eng., 1 (2020) 16-27. https://doi.org/10.37516/global.j.civ.eng.2020.012

[15] F. C Onyeka ,T. E Okeke, Analytical solution of thick rectangular plate with clamped and free support boundary condition using polynomial shear deformation theory, Advances in Science, Technol. Eng. Syst. J., 6 (2021) 1427-1439. https://doi.org/10.25046/aj0601162

[16] P. S. Gujar and K. B. Ladhane, Bending analysis of simply supported and clamped circular plate, Int. J. Civ. Eng., 2 (2015) 45-51. https://doi.org/10.14445/23488352/IJCE-V2I5P112

[17] F. C. Onyeka, Effect of Stress and Load Distribution Analysis on an Isotropic Rectangular Plate, Arid Zone J. Eng.Technol. Environ., 17 (2021) 9-26.

[18] F. C. Onyeka and T. E. Okeke, Analysis of critical imposed load of plate using variational calculus, J. Adv. Sci. Eng., 4 (2021) 13–23. https://doi.org/10.37121/jase.v4i1.125

[19] E. Reissner, The Effect of transverse shear deformation on the bending of elastic plates, J. Appl. Mech., 12 (1945) A69–A77. https://doi.org/10.1115/1.4009435

[20] M. Zenkour. Ashraf, Exact mixed-classical solutions for the bending analysis of shear deformable rectangular plates, Appl. Math. Model., 27 (2003) 515-534. https://doi.org/10.1016/S0307-904X(03)00046-5

[21] F. C. Onyeka, F. O. Okafor, H. N. Onah, Application of a new trigonometric theory in the buckling analysis of three-dimensional thick plate, Int. J. Emerg. Technol., 12 (2021) 228-240.

[22] Y. M. Ghugal, A. S. Sayyad, Free vibration of thick isotropic plates using trigonometric shear deformation theory, J. Solid Mech., 3 (2011) 172-182.

[23] A. S. Sayyad,Y. M. Ghugal, Bending and free vibration analysis of thick isotropic plates by using exponential shear deformation theory, Appl. Comput. Mech., 6 (2012) 65-82.

[24] F. C. Onyeka , D. Osegbowa, Stress analysis of thick rectangular plate using higher order polynomial shear deformation theory, FUTO J.Ser., 6 (2020) 142-161.

[25] I. I. Sayyad, Bending and free vibration analysis of isotropic plate using refined plate theory, Bonfring Int. J. Ind. Eng. Manag. Sci., 3 (2013) 40-46. https://doi.org/10.9756/BIJIEMS.4390

[26] F. C. Onyeka, Direct Analysis of critical lateral load in a thick rectangular plate using refined plate theory, Int.J.Civ. Eng.Technol., 10 (2019) 492-505.

[27] G. Kirchhoff, Ueber Die Schwingungen Einer Kreisförmigen Elastischen Scheibe, Annalen Der Physik, 157 (1850) 258-64. https://doi.org/10.1002/andp.18501571005

[28] F. C. Onyeka, T. E. Okeke, C. D. Nwa-David, Buckling analysis of a three-dimensional rectangular plates material based on exact trigonometric plate theory, J. Eng. Res. Sci., 1 (2022) 106-115. https://dx.doi.org/10.55708/js0103011

[29] F. C. Onyeka, B. O. Mama, T. E. Okeke, Exact three-dimensional stability analysis of plate using a direct variational energy method, Civ. Eng. J., 8 (2022) 60-80. http://dx.doi.org/10.28991/CEJ-2022-08-01-05

[30] M. Kashtalyan, Three-dimensional elasticity solution for bending of functionally graded rectangular plates, Eur. J .Mech. A Solids, 23 (2004) 853-864.

[31] F. C. Onyeka, D. Osegbowa and E. E. Arinze, Application of a new refined shear deformation theory for the analysis of thick rectangular plates, Nigerian Res. J. Eng. Environ. Sci., 5 (2020) 901-917.

[32] B. O. Mama, C. U. Nwoji, C. C. Ike and H. N. Onah, Analysis of simply supported rectangular kirchhoff plates by the finite fourier sine transform method, Int. J. Adv.Eng. Res. Sci.,4 (2017) 285-291. https://doi.org/10.22161/ijaers.4.3.44

[33] C. U. Nwoji, B. O Mama, C. C Ike and H. N. Onah, Galerkin-Vlasov method for the flexural analysis of rectangular Kirchhoff plates with clamped and simply supported edges, IOSR J. Mech. Civ. Eng.,14 (2017) 61-74. https://doi.org/10.9790/1684-1402016174

[34] N. N. Osadebe, C. C. Ike, H. N. Onah, C. U. Nwoji and F. O. Okafor, Application of Galerkin-Vlasov method to ,the flexural analysis of simply supported rectangular kirchhoff plates under uniform loads, Nigerian J. Technol ., 35 (2016) 732-738. https://doi.org/10.4314/njt.v35i4.7

[35] N. G. Iyengar (1988). Structural Stability of Columns and Plates, New York: Ellis Horwood Limited; 1988.

[36] D. P. Bhaskar, A. G. Thakur, I. I. Sayyad and S. V. Bhaskar, Numerical Analysis of Thick Isotropic and Transversely Isotropic Plates in Bending using FE Based New Inverse Shear Deformation Theory, Int. J. Automot. Mech. Eng., 18 (2021) 8882-8894. https://doi.org/10.15282/ijame.18.3.2021.04.0681

[37] A. S. Sayyad and Y. M. Ghugal, Bending and free vibration analysis of thick isotropic plates by using exponential shear deformation theory, Appl. Comput. Mech., 6 (2012) 65-82.

[38] Y. M. Ghugal and P. D. Gajbhiye, Bending analysis of thick isotropic plates by using 5th order shear deformation theory. J. Appl. Comput. Mech., 2 (2016) 80-95. https://doi.org/10.22055/jacm.2016.12366

[39] J. L. Mantari , C. G. Soares, Bending analysis of thick exponentially graded plates using a new trigonometric higher order shear deformation theory, Compos. Struct., 94 (2012) 1991-2000. https://doi.org/10.1016/j.compstruct.2012.01.005

[40] [40] F. C. Onyeka, T. E. Okeke . New Refined Shear Deformation Theory Effect on Non-Linear Analysis of a Thick Plate Using Energy Method, Arid Zone J. Eng. Technol. Environ., 17 (2021) 121-140.

[41] J. L. Mantari, A. S. Oktem, C. Guedes Soares, A new trigonometric shear deformation theory for isotropic, laminated composite and sandwich plates, Int. J. Solids Struct. 49 (2012) 43-53. http://doi.org/10.1016/j.ijsolstr.2011.09.008

[42] F. C. Onyeka, B. O. Mama and T. E. Okeke, Elastic bending analysis exact solution of plate using alternative i refined plate theory, Nigerian J. Technol.,40 (2021) 1018-1029. http://dx.doi.org/10.4314/njt.v40i6.4

[43] A.Y. Grigorenko, A. S. Bergulev, S. N. Yaremchenko Numerical solution of bending problems for rectangular plates, Int. Appl. Mech., 49 (2013) 81-94. https://doi.org/10.1007/s10778-013-0554-1

[44] F. C. Onyeka and B. O. Mama, Analytical study of bending characteristics of an elastic rectangular plate using direct variational energy approach with trigonometric function, Emerg. Sci. J., 5 (2021) 916-928. http://dx.doi.org/10.28991/esj-2021-01320

[45] F. C. Onyeka, T. E. Okeke and B. O. Mama, Static Elastic Bending Analysis of a Three-Dimensional Clamped Thick Rectangular Plate using Energy Method, HighTech Innov. J., 3 (2022) 267-281. http://dx.doi.org/10.28991/HIJ-2022-03-03-03

[46] F. C. Onyeka, T. E Okeke, Effect of load, shear and bending analysis of rectangular plate using polynomial displacement function, J. Res. Innov. Eng., 5 (2020) 145-158.

[47] Gwarah, L. S. Application of shear deformation theory in the analysis of thick rectangular plates using polynomial displacement functions. PhD Thesis Presented to the School of Civil Engineering, Federal University of Technology, Owerri, Nigeria, 2019.